Bio-Design and Manufacturing (2026) 9:599–611
https://doi.org/10.1631/bdm.2500511

RESEARCH ARTICLE

Subcutaneous microfuse-activated device for programmed pulsatile drug delivery

Myoung Ju Kim[1,2] · Han Bi Ji[1] · Yong Chan Cho[1] · Jae Chan Cho[1] · Woo Hyun Kim[1] · Gi Min Park[1,2] · Chang Hee Min[1] · Min Ji Kim[1] · Cho Rim Kim[1] · Jae Hoon Han[1] · Cheol Lee[3] · Mark R. Prausnitz[4] · Young Bin Choy[1,5,6,7,8]

Received: 7 October 2025 / Accepted: 12 January 2026 / Published online: 28 April 2026

Abstract

Pulsatile drug delivery, in which rapid drug release is separated by defined lag periods, offers significant therapeutic advantages but is limited by the need for repeated injections and poor patient adherence. Here, we introduce the fused device (FUSED), a subcutaneous system enabling programmed multidose drug delivery through a single implantation. FUSED comprises paired delay and shot units that regulate dosing intervals and trigger pulsatile drug release, respectively. After implantation, body fluids gradually dissolve the microfuse in each delay unit, with the delay duration determined by fuse length. Once fluid reaches a shot unit, an effervescent reaction is initiated, producing rapid drug release. In vitro and in vivo evaluations demonstrated precise pulsatile release of the model antigen ovalbumin, effectively reproducing prime–boost vaccination timing and eliciting the corresponding immune response. These results suggest that FUSED may provide a viable alternative to repeated injections and improve adherence in multidose therapeutic regimens.

Graphical abstract

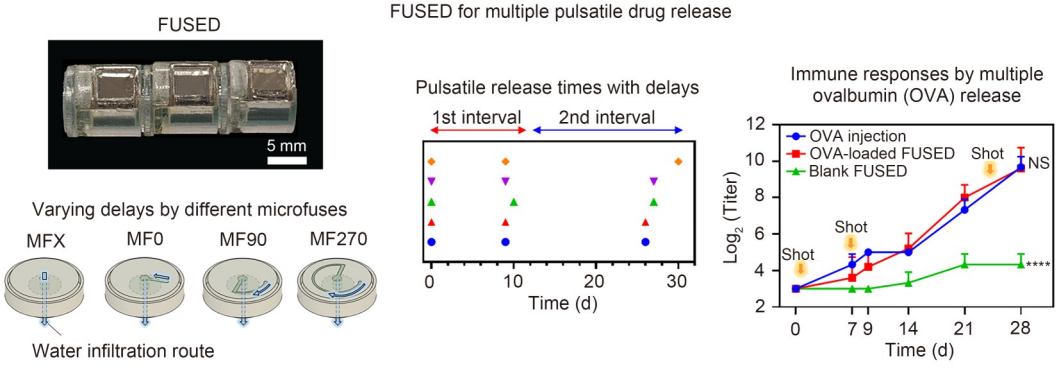

Keywords Implantable device · Microfuse · Actuator · Timed drug delivery · Pulsatile drug delivery

Myoung Ju Kim and Han Bi Ji have contributed equally to this work.

✉ Young Bin Choy
ybchoy@snu.ac.kr

1 Interdisciplinary Program for Bioengineering, College of Engineering, Seoul National University, Seoul 08826, Republic of Korea

2 Integrated Major in Innovative Medical Science, Seoul National University Graduate School, Seoul 03080, Republic of Korea

3 Department of Pathology, Seoul National University College of Medicine, Seoul 03080, Republic of Korea

4 School of Chemical and Biomolecular Engineering, Georgia Institute of Technology, Atlanta, GA 30332, USA

5 Institute of Medical and Biological Engineering, Medical Research Center, Seoul National University, Seoul 03080, Republic of Korea

6 Innovative Medical Technology Research Institute, Seoul National University Hospital, Seoul 03122, Republic of Korea

7 ToBIOS Inc., Seoul 02880, Republic of Korea

8 Department of Biomedical Engineering, Seoul National University College of Medicine, Seoul 03080, Republic of Korea

1 Introduction

In many therapeutic settings, certain diseases and physiological processes require drug administration at specific time points rather than maintenance of a constant systemic concentration to improve efficacy or minimize adverse effects. Pulsatile drug delivery, defined by rapid drug release interspersed with predetermined lag phases, can better synchronize with biological rhythms or time-dependent symptom onset. Accordingly, this approach has demonstrated advantages in applications such as vaccination, hormone therapy, treatment of psychotic disorders, and chronotherapy [1–7]. However, pulsatile delivery commonly relies on repeated injections administered at scheduled intervals, necessitating high patient adherence and/or involvement of trained healthcare personnel [8–11]. These requirements present substantial barriers to effective treatment, particularly for nonadherent populations and in resource-limited or remote settings [12].

To overcome these limitations, implantable devices capable of multidose drug delivery at predefined time points have been proposed as a promising alternative [13]. For clinical effectiveness, a single implantation must enable pulsatile drug release at multiple, preprogrammed intervals, thereby replicating conventional dosing regimens and optimizing therapeutic outcomes. Accordingly, a range of implantable systems—many based on microelectromechanical systems (MEMS)—have been developed that employ stimulus-responsive release mechanisms. These devices trigger drug release in response to external cues such as light [14, 15], magnetic fields [16, 17], wireless signals [18, 19], or ultrasound [20]. However, such approaches either require integrated electronic components, which increase device size, complexity, and cost, or depend on external stimulation equipment, thereby reducing patient convenience and overall practicality [21, 22].

Alternatively, implantable devices with core–shell structures have been proposed, in which the core contains the drug and the shell—composed of biocompatible polymers—encapsulates the drug [23–26]. In these systems, the polymer shell functions as a temporary barrier, delaying the onset of drug release as body fluids gradually dissolve or degrade the shell until the drug-containing core is exposed. This design allows for control over the interval between drug administrations. However, the polymer shell also acts as a diffusion barrier, leading to increasingly sustained drug release as the programmed interval lengthens. Consequently, achieving rapid and discrete pulsatile release at the intended dosing time becomes impractical, resulting in altered pharmacokinetics due to deviations from the intended dosing regimen [27].

To overcome these limitations, we propose an implantable device incorporating precisely tuned microfuses and actuators—hereafter termed the fused device (FUSED)—that enables multiple pulsatile drug releases exclusively at preprogrammed time points. FUSED consists of two primary functional units arranged in series: a delay unit and a shot unit. The delay unit houses a time-delay microfuse, while the shot unit contains a drug reservoir and an actuator.

In this study, we developed a FUSED comprising three discrete delay–shot unit pairs, each loaded with the model antigen ovalbumin (OVA), to assess the feasibility of delivering multiple pulsatile doses at predefined intervals. The delay units were engineered with microfuses of different lengths to enable autonomous drug release on Days 0, 7, and 28 after implantation, thereby recapitulating standard vaccination schedules used for infectious diseases such as rabies, hepatitis, and Japanese encephalitis [28–30]. To establish the required delay durations, delay units incorporating microfuses of varying lengths were first characterized under in vitro conditions. The selected configurations were then integrated into a single FUSED for subsequent in vivo evaluation.

2 Experimental section

2.1 Materials

Veroclear and SUP706 resins for three-dimensional (3D) printing were purchased from Stratasys (Rehovot, Israel). Medical-grade epoxy (EPO-TEK® 301-2) and a titanium membrane (2-μm thickness) were obtained from Epoxy Technology (Billerica, MA, USA) and Nilaco (Tokyo, Japan), respectively. Medical-grade stainless-steel plates (SUS316L) were purchased from SKB TECH (Ulsan, Republic of Korea), and polymethyl methacrylate (PMMA) plates were obtained from ENGP (Incheon, Republic of Korea). Polyethylene glycol (PEG; average molecular weight: 35 kDa), fluorescein sodium salt, sodium bicarbonate, polyvinyl alcohol (PVA), and OVA (lyophilized powder, >98%) were purchased from Sigma-Aldrich (St. Louis, MO, USA). Ascorbic acid and starch were obtained from Daejung Chemicals (Siheung, Republic of Korea) and Colorcon (Harleysville, PA, USA), respectively. Formalin was purchased from Thermo Fisher Scientific (Waltham, MA, USA). Ideal 9144 silicone tape was obtained from American Biltrite (Wellesley Hills, MA, USA). L929 cells were obtained from the Korea Cell Line Bank (Seoul, Republic of Korea). A rat OVA-specific immunoglobulin G (IgG) enzyme-linked immunosorbent assay (ELISA) kit was purchased from FineTest (Hubei, China).

2.2 FUSED fabrication

The individual components of FUSED were designed using Autodesk Fusion 360 (Autodesk, Mill Valley, CA, USA)

and fabricated using a 3D printer (Object30 Pro, Stratasys, Rehovot, Israel). The printed parts were assembled with medical-grade epoxy, as shown in Fig. 1a. To fabricate the delay unit, a microfuse pattern was laser-etched onto the top surface of a PMMA plate (8-mm diameter and 1-mm thickness) using a CO_2 laser system (Universal Laser ILS12.150 D, Universal Laser Systems, Scottsdale, AZ, USA). The microfuse channel was etched at a scanning speed of 500 mm/s and a laser power of 84 W. A central through-hole was subsequently formed at a scanning speed of 100 mm/s and a laser power of 72 W. The patterned PMMA plate was bonded to the bottom cover, after which the microfuse channel and through-hole were filled with molten PEG, a biocompatible polymer [31, 32], using a syringe at 100 °C. The assembled unit was placed in an oven overnight to allow the PEG to cool to 25 °C and solidify. Subsequently, a permeable film and a unit connector were attached to the underside of the bottom cover. The top surface of the microfuse was then sealed with Ideal 9144 silicone tape, leaving the microfuse opening exposed (Fig. S1 in the supplementary information). In this study, four types of delay units—designated MFX, MF0, MF90, and MF270—were fabricated, each distinguished by a different microfuse length. The selected lengths were initially determined based on our previous studies [33–35].

For the shot unit, an inflatable membrane was fabricated by thermoforming a 0.2-mm-thick polyurethane film at 100 °C for 10 min into a convex geometry and subsequently bonding it to an air chamber. A needle holder was mounted on the inflatable membrane, into which a needle tip (1.1-mm length) was securely fixed. A test compound—either fluorescein (20 mg/mL) or OVA (2 mg/mL)—was dissolved in an aqueous 2% (20 g/L) PVA solution. A 5-µL aliquot of this solution was dispensed into the concave space above the inflatable membrane and freeze-dried overnight (model 793404, Labconco, Kansas City, MO, USA) to form the drug reservoir. An effervescent tablet (2.8-mm diameter and 0.8-mm height) was prepared by compressing a powder mixture of ascorbic acid, sodium bicarbonate, and starch (binder) at a weight ratio of 1 : 1 : 0.4 (ascorbic acid:sodium bicarbonate:starch). The effervescent tablet was placed within an effervescent container. The drug reservoir and effervescent container were then integrated into the device housing, and the reservoir was sealed with a sealing membrane and top cover. Finally, the delay and shot units were joined and bonded via the unit connector at

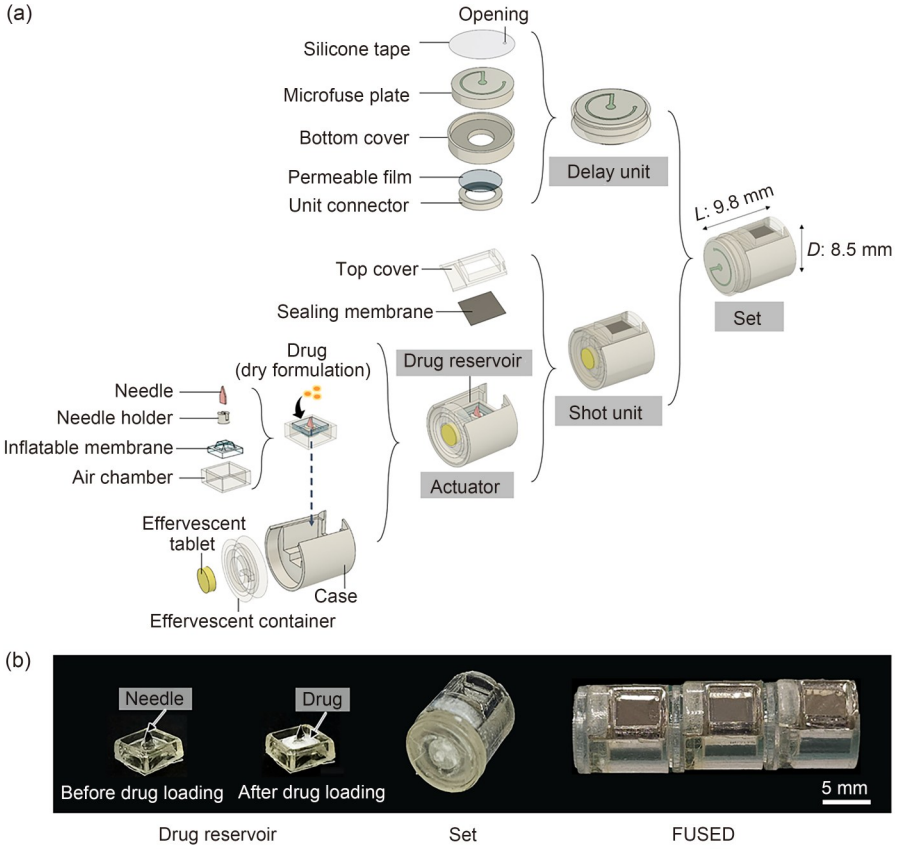

Fig. 1 Design of FUSED and its components. (a) Schematic illustration showing an exploded view of a single set composed of a delay unit and a shot unit connected in series. (b) Optical images of the drug reservoir, an individual set, and a complete FUSED device assembled with three distinct sets. *L*: height of a set; *D*: diameter of a set

the permeable-membrane interface to form a single functional set. Multiple such sets were subsequently connected in series to fabricate the final FUSED device.

2.3 In vitro performance testing

To evaluate device performance under in vitro conditions, either a single set or a complete FUSED device loaded with fluorescein was fully immersed in phosphate-buffered saline (PBS; pH 7.4) at 37 °C. Immersion volumes were 5 mL for a single set and 15 mL for the full FUSED device. To determine the onset day of drug release, a fixed volume of PBS (2.5 mL for a single set and 10 mL for FUSED) was collected once daily and replaced with an equal volume of fresh PBS. Collected samples were analyzed using an ultraviolet–visible (UV–vis) spectrophotometer (UV-1800, Shimadzu, Kyoto, Japan) at 321 nm to quantify released fluorescein. The onset day of drug release was defined as the time point at which a stepwise increase in cumulative release, comparable to the dose loaded in a single set, was observed. The release interval was defined as the elapsed time between two successive onset days. Five individual sets were tested for each microfuse type, and five complete FUSED devices were evaluated. To characterize immediate in vitro drug release following actuation, five MFX sets (i.e., shot units lacking a microfuse) were individually immersed in 5 mL of PBS (pH 7.4) at 37 °C. At 10-min intervals, 2.5 mL of the release medium was collected and replaced with an equal volume of fresh PBS.

2.4 Cytotoxicity

To evaluate the biocompatibility of FUSED, an indirect cytotoxicity assay was conducted as previously described [35, 36]. A blank FUSED device, sterilized with ethylene oxide, was fully immersed in 4 mL of culture medium (RPMI 1640 supplemented with 10% fetal bovine serum, 100 U/mL penicillin, and 100 μg/mL streptomycin) and incubated at 37 °C in a humidified atmosphere containing 5% CO_2 for 28 d. At predetermined time points, the extraction medium was completely collected and replaced with an equal volume of fresh medium. The collected extracts were used to assess cytotoxicity in L929 mouse fibroblast cells. Briefly, 1.0×10^4 cells were seeded into each well of a 96-well plate and incubated at 37 °C under 5% CO_2 for 24 h. Subsequently, 100 μL of the collected extraction medium was added to each well and incubated for an additional 24 h. The medium was then replaced with fresh medium, followed by the addition of 10 μL of EZ-Cytox reagent and incubation for 2 h. Absorbance was measured at 450 and 600 nm using a microplate reader (SpectraMax 190, Molecular Devices, San Jose, CA, USA). Cell viability was calculated as follows:

$$\text{Cell viability} = \frac{A_{450\text{t}} - A_{600\text{t}}}{A_{450\text{ut}} - A_{600\text{ut}}} \times 100\%, \quad (1)$$

where $A_{450\text{t}}$ and $A_{600\text{t}}$ represent the absorbance of treated wells at 450 nm and 600 nm, respectively, and $A_{450\text{ut}}$ and $A_{600\text{ut}}$ represent the absorbance of untreated control wells at 450 nm and 600 nm, respectively [36].

2.5 In vivo performance test

All animal experiments were performed using 7-week-old male Sprague–Dawley rats (Orient Bio, Seongnam, Republic of Korea) in accordance with institutional guidelines approved by the Institutional Animal Care and Use Committee of the Seoul National University Hospital Biomedical Research Institute (IACUC number: 23-0048-S1A1). Animals were housed in a pathogen-free facility under controlled temperature and humidity conditions with a 12:12 h light/dark cycle. Prior to implantation, all FUSED devices were sterilized using ethylene oxide gas and implanted into subcutaneous pockets, as shown in Fig. S2 (supplementary information).

To monitor in vivo actuation of FUSED, micro-computed tomography (micro-CT) images were acquired every 2 d after implantation (Quantum GX2, PerkinElmer, Waltham, MA, USA). For imaging, rats were anesthetized via intraperitoneal injection of alfaxalone (10 mg/kg) and xylazine (5 mg/kg) [37]. The implantation sites were scanned using an X-ray source voltage of 90 kV and a current of 88 μA. Tomographic datasets were acquired and reconstructed using Quantum GX2 image analysis software (PerkinElmer). Needle position was monitored in cross-sectional images of the implanted FUSED devices; upward displacement from the initial position indicated rupture of the sealing membrane and was defined as the onset of drug release. To evaluate the immunization efficacy of FUSED, rats were randomly assigned to three experimental groups: (1) an OVA injection group (n=3), in which rats received subcutaneous OVA injections; (2) an OVA-loaded FUSED group (n=5), in which rats were implanted with FUSED devices containing OVA; (3) a blank FUSED group (n=3), in which rats were implanted with FUSED devices without OVA. Each set within the OVA-loaded FUSED contained 10 μg of OVA. Rats in the OVA injection group received 10 μg of OVA via subcutaneous injection on Days 1, 7, and 25, whereas animals in the OVA-loaded FUSED and blank FUSED implantation groups received no additional treatment after implantation. For all groups, 1 mL of blood was collected from the lateral tail vein using heparin-coated hematocrit tubes (Kimble-Chase, Vineland, NJ, USA) on Days 0, 7, 9, 14, 21, and 28. Blood samples were centrifuged at 2000 r/min for 10 min to isolate serum, which was subsequently stored at −20 °C until further analysis [38].

Total OVA-specific IgG levels in serum were quantified using a commercial ELISA kit (FineTest, Hubei, China). Briefly, antigen-precoated 96-well plates were washed twice with wash buffer, after which 100 μL of prepared standards or diluted serum samples were added to each well. Plates were sealed and incubated at 37 °C for 90 min. After three washes, 100 μL of horseradish peroxidase-conjugated antibody working solution was added to each well, and the plates were incubated for an additional 30 min at 37 °C. Plates were then washed five times, and 90 μL of 3,3',5,5'-tetramethylbenzidine (TMB) substrate solution was added. After incubation for 15 min at 37 °C, the reaction was terminated by adding 50 μL of TMB stop solution. Optical density at 450 nm (OD450) was immediately measured using a microplate reader. Antibody titers were expressed as the $\log_2$ value of the dilution factor corresponding to the lowest concentration that produced an OD450 exceeding that of the blank control. Each sample was analyzed in duplicate to minimize experimental variability.

2.6 Histology

For histopathological analysis, animals implanted with OVA-loaded FUSED devices were euthanized by CO_2 inhalation at the end of the study. Tissues surrounding the implants were harvested, fixed in 4% paraformaldehyde for 24 h, and embedded in paraffin. Paraffin blocks were sectioned into 4-μm-thick slices and stained with hematoxylin and eosin (H&E). Stained sections were examined by a professional pathologist (C. L.) using an optical microscope (BX53, Olympus, Tokyo, Japan).

2.7 Statistical analysis

Data are presented as mean±standard deviation. Statistical analyses were conducted using GraphPad Prism 7 (GraphPad Software, San Diego, CA, USA). Differences among groups were assessed by two-way analysis of variance with repeated measures. Statistical significance was defined as $p<0.0001$.

3 Results

3.1 FUSED fabrication and working principles

In this study, FUSED was fabricated by assembling multiple cylindrical sets, each comprising a delay unit and a shot unit connected in series (Fig. 1). All components were designed and fabricated via 3D printing (Object30 Pro, Stratasys). Within the shot unit, a dry OVA formulation (10 μg) was loaded into the drug reservoir, which was hermetically sealed at the top with a 2-μm-thick titanium membrane. The actuator was separated from the reservoir by a polyurethane inflatable membrane, to which a needle was attached and positioned within the reservoir. In the unactuated state, the inflatable membrane remained relaxed, maintaining separation between the needle tip and the sealing membrane to prevent drug release. Beneath the inflatable membrane, an air chamber was connected to an effervescent container housing a tablet composed of ascorbic acid and sodium bicarbonate. Upon contact with water, ascorbic acid dissolved to form an acidic solution, which reacted with sodium bicarbonate to generate CO_2 gas [39, 40].

In the delay unit, a microfuse was patterned on the surface of a plate, and a central through-hole was fabricated; both features were filled with PEG. The top surface of the plate was sealed with a silicone tape containing an opening aligned with the initial point of the microfuse, enabling controlled water infiltration. A permeable film was positioned at the interface between the delay and shot units to allow water access to the effervescent formulation while preventing backflow of generated gas. In this study, a single set measured 8.5 mm in diameter and 9.8 mm in length. Accordingly, the representative FUSED device comprised three sets connected in series, yielding an overall diameter of 8.5 mm and a length of 29.4 mm.

Figure 2a illustrates the working principle of the delay unit. When water reaches the inlet opening, it infiltrates through the microfuse by gradually dissolving the PEG, progressing toward the central through-hole. The microfuse has a cross-sectional area of 0.037 μm^2, whereas the cross-sectional area of the central through-hole is substantially larger (0.79 mm^2). As a result, water infiltration through the microfuse dominates the delay process, whereas transport through the through-hole contributes negligibly to the overall delay. To modulate the delay duration, we designed four different types of delay units, as shown in Fig. 2b: MFX, MF0, MF90, and MF270. The MFX contained only a central through-hole and no microfuse. In MF0, the microfuse extended radially outward from the center. In MF90 and MF270, the microfuse initially extended radially from the

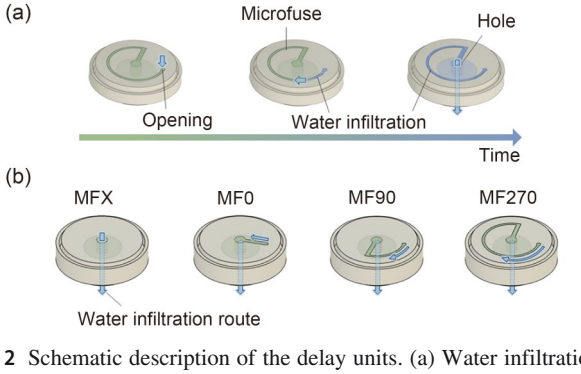

Fig. 2 Schematic description of the delay units. (a) Water infiltration process through a microfuse. (b) Four types of delay units with different programmed delay times fabricated in this study

center and then followed the circular perimeter to angles of 90° and 270°, respectively.

A delay unit combined with the shot unit formed a single set, and a FUSED composed of multiple sets connected in series is shown in Fig. 3a. Following subcutaneous implantation, body fluid infiltrates the microfuse of Set 1, triggering the programmed time delay (Fig. 3b). The fluid subsequently passes through the permeable film and contacts the effervescent tablet, initiating dissolution and CO_2 gas generation (Fig. 3c). Gas generation increases pressure within the air chamber, causing the inflatable membrane to expand and the needle to be displaced upward, rupturing the sealing membrane (Fig. 3d). Body fluid then enters the drug reservoir, rapidly dissolving the dry drug formulation and releasing the resulting solution into the surrounding tissue (Fig. 3e). Concurrently, body fluid within the drug reservoir begins to infiltrate the microfuse opening of Set 2, thereby initiating the same sequence of events (Fig. 3f). Accordingly, each release interval can be independently programmed through the specific microfuse design of each set. Rapid and discrete pulsatile drug release is achieved through swift exposure of the drug reservoir to body fluid following mechanical rupture of the sealing membrane by the actuator.

3.2 In vitro performance

To evaluate the performance of the delay and shot units, four types of sets were prepared, each comprising a shot unit connected to a delay unit with one of four microfuse

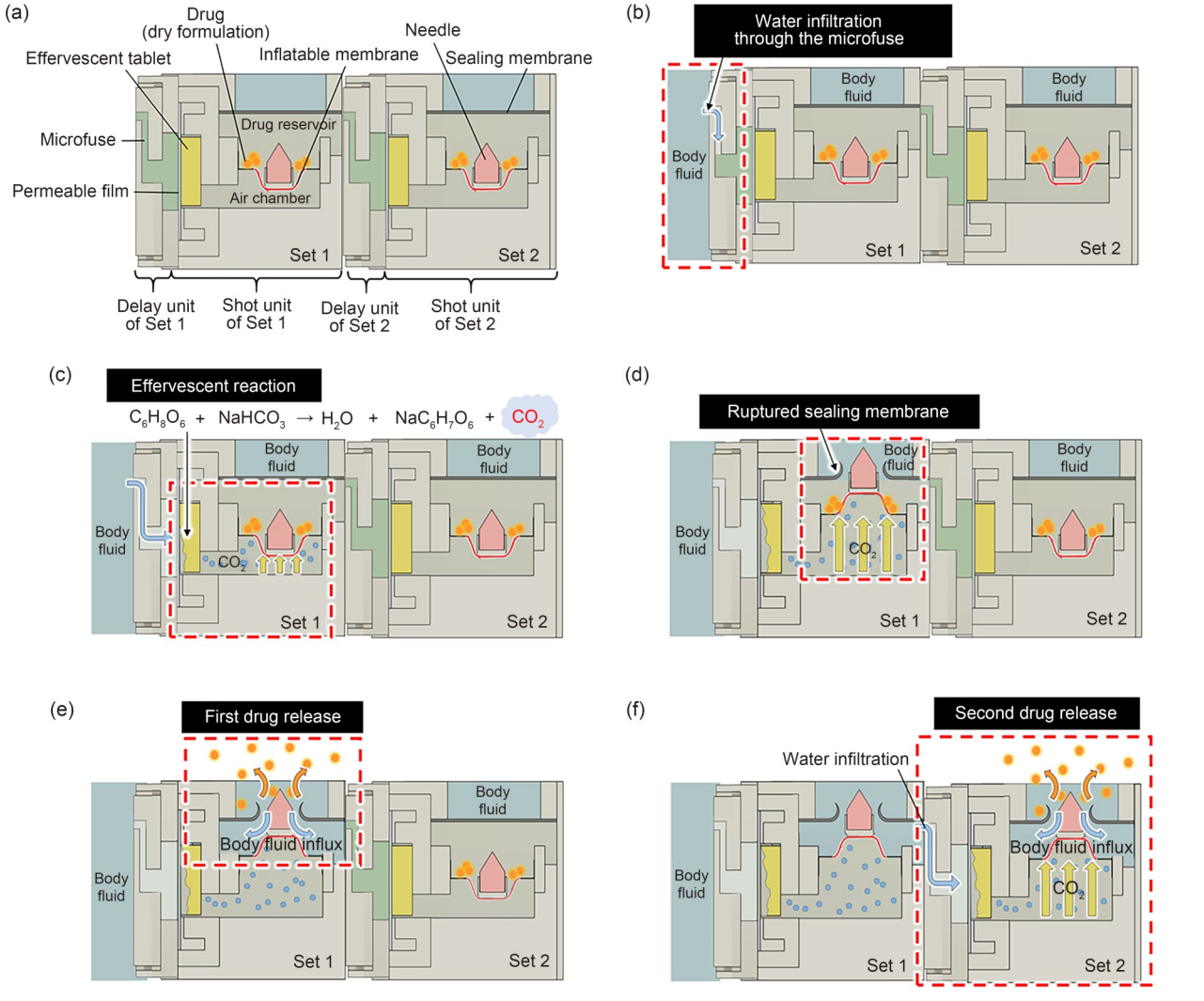

Fig. 3 Schematic illustration of the working principle of FUSED, shown as a cross-sectional view of two sets connected in series. (a) Before water infiltration, the inflatable membrane remains relaxed, and the needle does not contact the sealing membrane. (b) After implantation, body fluid infiltrates the microfuse, creating a programmed time delay. (c) When body fluid reaches the effervescent tablet, CO_2 gas is generated. (d) The resulting pressure increase expands the inflatable membrane, driving the needle to rupture the sealing membrane. (e) When body fluid reaches the drug reservoir, it dissolves the drug and enables its release through the ruptured sealing membrane. (f) Body fluid within the drug reservoir of Set 1 subsequently infiltrates the microfuse of Set 2, initiating the next release cycle

configurations: MFX, MF0, MF90, or MF270 (Fig. 2b). Each set was loaded with fluorescein as a model compound and immersed in PBS (pH 7.4) at 37 °C. Figure 4a shows the onset time of drug release, measured across five independent sets for each microfuse configuration. As the microfuse length increased, the onset time of dye release correspondingly increased [33, 34, 36]. At each onset time, rupture of the sealing membrane was observed for all device configurations (see also Sect. S1 in the supplementary information).

Specifically, the mean onset time for the MFX, MF0, MF90, and MF270 sets was 0, (4.0±0.71), (8.2±0.45), and (16.6±0.89) d, respectively. Variability among the five sets within each configuration was minimal, with all onset times falling within ±1 d of the median. For the MFX set, which lacked a microfuse, the sealing membrane ruptured within 1 h, and complete drug release occurred within the subsequent hour (Fig. 4b). This release profile confirms the rapid and discrete pulsatile drug release driven by the actuator within the shot unit.

In this study, we aimed to demonstrate pulsatile drug delivery using FUSED by administering an antigen in multiple discrete doses at preprogrammed time points. To guide device design, we referenced established vaccination schedules requiring three doses on Days 0, 7, and 28 [30, 41]. This regimen entails two dosing intervals: approximately 7 d between the first and second doses and 21 d between the second and third doses. Accordingly, FUSED was configured with three serially connected sets incorporating MFX, MF90, and MF270 delay units, providing approximate delays of 0, 8, and 17 d, respectively (Fig. 4a). When connected in series, these delays accumulated sequentially, yielding expected antigen release on Days 0, 8, and 25.

As shown in Fig. 4c, all five FUSED devices fabricated in this study exhibited three distinct pulsatile drug release events occurring on Days 0, 9.2±0.44, and 27.2±1.64, respectively. The corresponding intervals between releases were (9.2±0.44) and (18.0±1.22) d, which closely matched the delays predicted for the MF90 and MF270 units, respectively. Variability in pulsatile release timing was minimal,

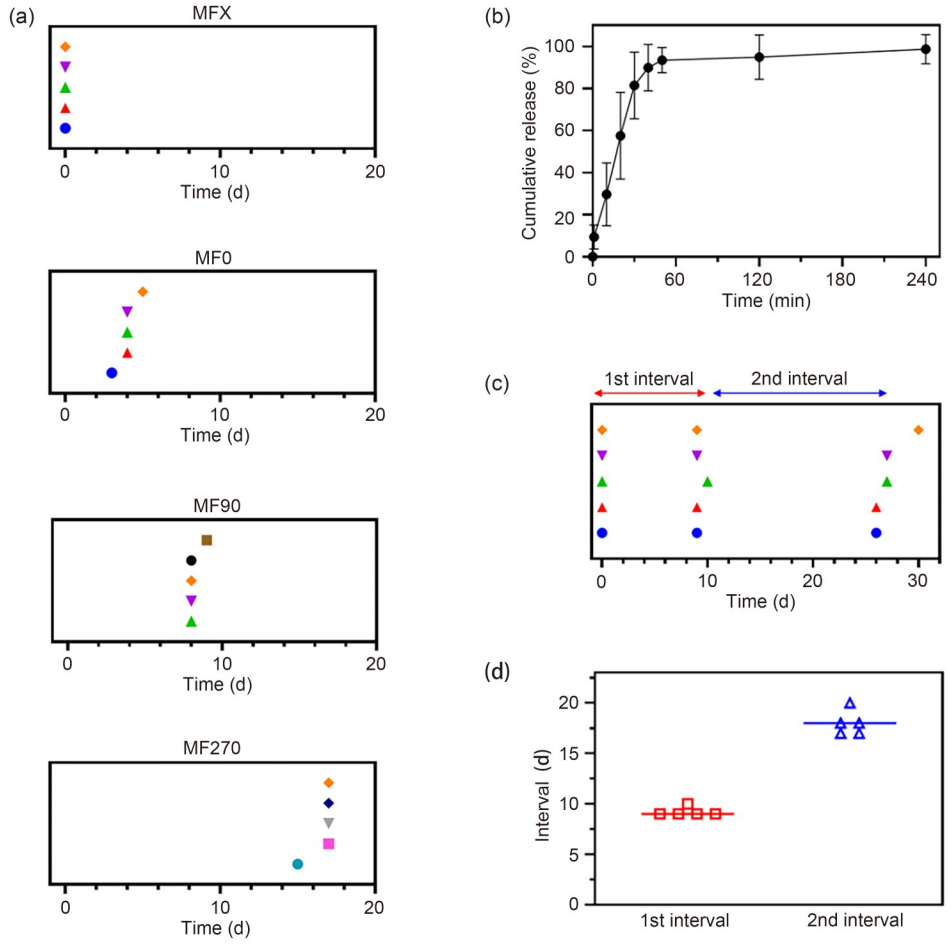

Fig. 4 In vitro performance of sets incorporating four different microfuse configurations. (a) Onset days of drug release were measured from five independent sets for each microfuse type. (b) Drug release profile obtained from the MFX set immediately after actuation. Error bars represent the standard deviation (n=5). Onset days of drug release (c) and intervals between successive release events (d) from five FUSED devices assembled by serially connecting MFX, MF90, and MF270 sets

with all values falling within ±2 d of the median. The second and third release times observed for the three-set FUSED devices (Figs. 4c and 4d) were slightly longer than those measured using individual sets (Fig. 4a). This difference is likely attributable to additional resistance to water diffusion through the upstream sets, even after their microfuse channels have opened. Such effects can be accommodated in future FUSED designs by proportionally reducing the length of the corresponding microfuse channels.

Prior to the in vivo experiments, the cytotoxicity of FUSED devices was evaluated by exposing L929 fibroblast cells to the extraction medium in which the devices had been immersed [35, 36]. No cytotoxic effects were observed, confirming the biocompatibility of the devices (Fig. S3 in the supplementary information).

3.3 In vivo performance

To assess the in vivo performance of multiple pulsatile drug deliveries, FUSED devices with each shot unit loaded with OVA (10 μg) were subcutaneously implanted in rats (Fig. S2 in the supplementary information). At predetermined time points, actuation of each shot unit was monitored via needle displacement using micro-CT imaging (Quantum GX2, PerkinElmer). Upward movement of the needle indicated rupture of the sealing membrane and the onset of drug release. As shown in Fig. 5a, immediately after implantation (Day 0), the needles in all three sets remained in their initial positions beneath the sealing membrane. On Day 1, upward displacement of the needle was observed in Set 1, which contained the MFX delay unit, whereas the needles in Sets 2 and 3 remained stationary. Subsequent needle movements occurred on Days 7 and 25 for Sets 2 and 3, respectively. These in vivo actuation time points closely corresponded to the pulsatile release events observed in vitro (Fig. 4), although the delays were slightly shorter for the three-set FUSED device. This discrepancy may reflect differences in microfuse dissolution kinetics between PBS used in vitro and subcutaneous body fluid in vivo.

The in vivo pharmacodynamic efficacy of OVA delivery via FUSED was further assessed by measuring OVA-specific IgG titers [42, 43]. Responses were compared with those in rats receiving multiple subcutaneous injections of the same OVA dose on Days 1, 7, and 25. As shown in Fig. 5b, a single implantation of FUSED elicited robust OVA-specific IgG responses, with magnitudes comparable to those observed in rats receiving three scheduled subcutaneous injections.

In contrast, implantation of a blank FUSED device without OVA did not elicit any anti-OVA immune response. Collectively, these results demonstrate that FUSED can effectively replicate a multidose injection regimen through a single implantation, underscoring its potential for preprogrammed, scheduled drug delivery and vaccination.

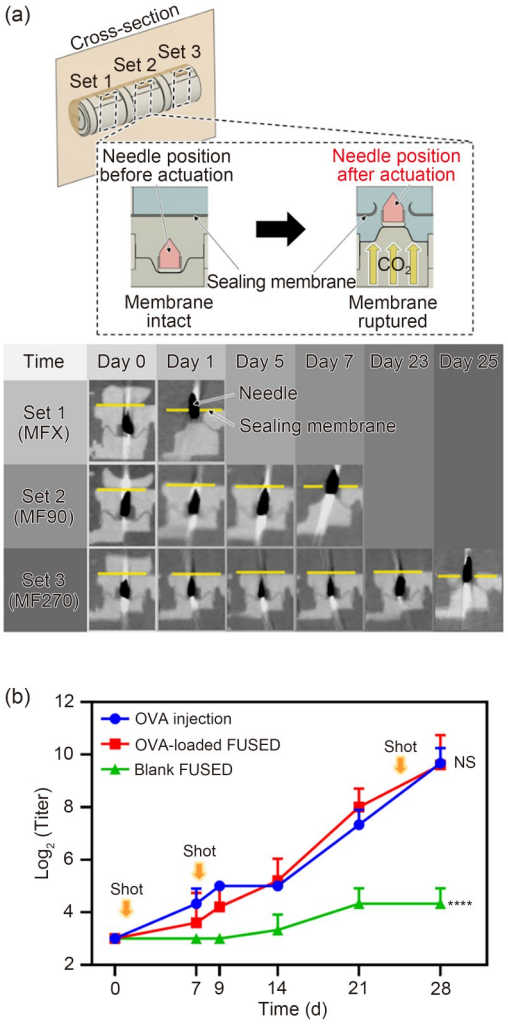

Fig. 5 In vivo performance of FUSED devices. (a) Representative micro-CT images of FUSED devices at scheduled time points following subcutaneous implantation in rats (n=3). Changes in needle position for each set indicate the timing of actuation. (b) Immune responses were assessed by measurement of OVA-specific IgG titers in three different animal groups: OVA injection (n=3), OVA-loaded FUSED (n=5), and blank FUSED (n=3). Error bars represent the standard deviation. $^{****}p<0.0001$ indicates a significant difference between OVA-loaded FUSED and blank FUSED; NS indicates no significant difference between OVA-loaded FUSED and OVA injection

To evaluate biocompatibility, tissues surrounding the implanted FUSED devices were harvested after completion of drug delivery and analyzed by H&E staining. As shown in Fig. 6, FUSED implantation induced a mild inflammatory response, accompanied by a fibrotic tissue layer surrounding the device. These responses were consistent with previously reported observations for similar implantable devices [35, 44]. No additional abnormalities were detected, in line with the established biocompatibility of the materials used in FUSED [32, 45].

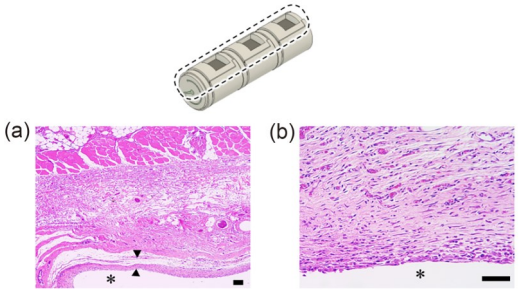

Fig. 6 Representative hematoxylin and eosin (H&E)-stained histological images of tissues surrounding the FUSED 45 d after implantation. Tissue samples were collected adjacent to the sealing membrane from rats implanted with FUSED devices and examined using an optical microscope at 40× (a) and 200× (b) magnification. Asterisks (*) indicate the location of the FUSED. Scale bars: 100 μm

4 Discussion and conclusions

Certain diseases and conditions require multiple pulsatile drug administrations, typically achieved through repeated injections at fixed intervals [6, 7]. This approach presents substantial challenges related to patient adherence and accessibility, particularly due to the need for precise timing and reliable administration. A single device capable of delivering multiple drug pulses at predetermined time points would therefore offer considerable clinical advantages. Implantable systems enabling autonomous, time-programmed pulsatile drug release represent an attractive solution; however, many previously developed devices have exhibited unintended drug leakage between doses or increasingly prolonged release profiles as the intervals between successive administrations lengthened [23, 24, 26, 46].

In this study, we introduced an implantable device—referred to as FUSED—that addresses these limitations through precise temporal control of drug release. In FUSED, microfuse length governs the time period of water infiltration, after which infiltrating water initiates an effervescent reaction that activates the actuator and ruptures the sealing membrane, resulting in rapid bolus release (Figs. 2 and 3). The rate of water infiltration is controlled by the dissolution of the water-soluble polymer PEG through microfuses of defined lengths. By serially connecting multiple delay units, we demonstrated the feasibility of delivering multiple drug doses with timing accuracy within ±2 d of the intended median. Further optimization of microfuse dimensions or the use of alternative polymers with higher or lower resistance to water diffusion could provide broader flexibility in modulating the delay between successive drug administrations [47–50].

The tunable microfuse allows customization of the FUSED system for applications requiring multiple bolus drug administrations over extended intervals, including treatments for psychological, immunological, and metabolic disorders. For example, to match the administration schedule of the Bacillus Calmette–Guérin vaccine, used in melanoma treatment and given once weekly for 3 weeks [51], a FUSED configuration comprising three sets with MF90 delay units may be suitable. Similarly, therapeutics such as alirocumab, tocilizumab, and risperidone, which require multiple doses at 1–2-week intervals, could be delivered using MF90 or MF270 delay units to align with optimized dosing schedules [52–54]. By enabling diverse combinations of dosing intervals, the modular design of FUSED supports tailored therapeutic regimens across multiple disease targets. This delivery flexibility enhances adaptability and advances personalized medicine [55].

The actuator design presented herein enables abrupt rupture of the sealing membrane, facilitating rapid and discrete pulsatile drug release. This behavior is driven by an effervescent reaction in combination with a specifically engineered inflatable membrane that serves as a mechanical trigger. In this system, infiltrating water functions like a burning spark traveling along a fuse; upon reaching the effervescent formulation, CO_2 gas is generated and accumulates within the air chamber, gradually exerting pressure on the inflatable membrane and storing mechanical strain energy. Once the accumulated strain energy exceeded a critical threshold, the relaxed, concave inflatable membrane rapidly transitioned to a convex configuration, releasing the stored energy [56, 57]. This rapid mechanical transition generated sufficient kinetic energy to propel the attached needle upward, instantly rupturing the sealing membrane. Subsequent inflation of the membrane allowed body fluid to enter the drug reservoir, initiating rapid pulsatile drug release [58], which was completed within 1 h (Fig. 4b). This release behavior contrasts with that of previously reported systems designed for multiple drug deliveries at programmed intervals, which typically exhibited sustained-release profiles with prolonged release durations between administrations [23, 24, 26, 35, 46, 59]. Rapid drug release following membrane rupture is also expected to occur in vivo; however, additional studies are required to confirm this behavior under physiological conditions. Notably, actuation of the inflatable membrane was governed solely by the pressure difference between the drug reservoir and the air chamber within the device, preventing external forces from triggering unintended needle deployment.

Since body fluid serves as the dissolution medium for both actuation and drug release, this design enables the use of dry formulations, thereby enhancing the long-term stability required for a broad range of therapeutics [60, 61]. Consequently, the rapid release kinetics achieved with FUSED is expected to preserve the intrinsic pharmacokinetic profile of administered drugs, supporting adaptability across diverse disease indications [60, 61]. In addition, the ability of FUSED to load dry formulations enables the incorporation

of sustained-release drug metrics, enabling more precise tailoring of release kinetics to meet therapeutic requirements. For instance, by loading a 3-week sustained-release formulation of progestin and estrogen incorporating a 1-week drug-free interval through a delay unit, the FUSED device could replicate the pharmacokinetic profile of bihormonal contraception. Such a configuration would preserve the scheduled hormone-free window and may reduce menstrual cycle disruptions commonly associated with continuous hormone dosing [62, 63].

Although the current FUSED prototype demonstrated effective multipulsatile drug delivery (Fig. 5), several enhancements are required to further advance its clinical translation. The current FUSED design has dimensions comparable to those of clinically approved implantable devices [64, 65]; however, further miniaturization—particularly a reduction in device diameter—along with improved reproducibility of the microfuses would enhance its clinical translatability. These improvements could be achieved through advanced manufacturing approaches, including microinjection molding, hot embossing with wafer-level alignment, and MEMS lithography on polymer substrates, which offer increased fabrication precision and reproducibility [66–68]. Furthermore, established microfluidic fabrication techniques, such as solvent bonding, thermal fusion, and automated assembly, could be adopted to improve hermetic sealing and enhance dimensional stability [66, 69–71]. Moreover, all constituent materials could be substituted with biodegradable polymers [69, 72] or metals [73] to maintain biocompatibility while eliminating the need for device retrieval.

Effective treatment with multidose regimens requires precise control of dosing intervals and rapid drug administration at each scheduled time point, ideally via pulsatile release. In this study, we demonstrated a subcutaneous implantable device, FUSED, capable of delivering multiple pulsatile drug doses through a single administration. FUSED integrates a series of paired delay and shot units, with each delay unit containing a microfuse that functions as a programmable timer—the microfuse length determining the delay before body fluid infiltration. Once fluid reaches the shot unit, it activates an effervescent actuator that generates CO_2 gas, triggering rapid drug release at the intended time point. Although this study evaluated a model vaccine in a relatively small cohort, FUSED elicited immune responses comparable to those achieved with multiple scheduled injections. These results suggest that FUSED may provide a promising alternative to conventional drug delivery approaches.

In conclusion, FUSED represents a promising long-acting pulsatile drug delivery system with the potential to replace multiple bolus injections and improve patient adherence, ultimately contributing to the prevention of millions of fatal infections. Moreover, this study establishes a foundation for the development of implantable, programmable drug delivery systems with broad applications in vaccination and other therapeutic areas.

Supplementary Information The online version contains supplementary material available at https://doi.org/10.1631/bdm.2500511.

Acknowledgements This work was supported by the National Research Foundation of Korea (NRF) grant funded by the Korea government (MSIT) (Nos. RS-2025-00555398 and RS-2024-00410364).

Author contributions Conceptualization: MJK (Myoung Ju Kim), HBJ, MRP, and YBC. Methodology: MJK (Myoung Ju Kim), HBJ, YCC, JCC, WHK, GMP, CHM, MJK (Min Ji Kim), CRK, JHH, CL, MRP, and YBC. Investigation: MJK (Myoung Ju Kim), HBJ, YCC, CHM, MJK (Min Ji Kim), CRK, JHH, CL, MRP, and YBC. Data curation: MJK (Myoung Ju Kim), HBJ, and CL. Formal analysis: MJK (Myoung Ju Kim) and HBJ. Resources: MJK (Myoung Ju Kim) and HBJ. Software: MJK (Myoung Ju Kim) and HBJ. Validation: MJK (Myoung Ju Kim), HBJ, and CL. Visualization: MJK (Myoung Ju Kim) and HBJ. Supervision: YBC. Funding acquisition: YBC. Project administration: YBC. Writing—original draft: MJK (Myoung Ju Kim), HBJ, MRP, and YBC. Writing—review & editing: MJK (Myoung Ju Kim), HBJ, CL, MRP, and YBC.

Funding Open access funding enabled and organized by Seoul National University.

Declarations

Conflict of interest YBC, MJK (Myoung Ju Kim), HBJ, and YCC are listed as inventors on the patent application (PCT/KR2025/005207 and KR 10-2024-157002) filed by Seoul National University Research & Development Business (SNU R&DB) for the device described in this article. The other authors declare that they have no conflict of interest.

Ethical approval All animal experimental procedures in this study were performed in accordance with institutional guidelines approved by the Institutional Animal Care and Use Committee at Seoul National University Hospital Biomedical Research Institute (IACUC number: 23-0048-S1A1).

Data availability Data supporting the findings of this study are available within this article and its supplementary information files and from the corresponding author upon reasonable request.

Use of generative AI tools ChatGPT was used only for grammar check during the preparation of this manuscript. After using this tool, the authors reviewed and edited the content as needed and take full responsibility for the content of the publication.

References

1. Filicori M, Cognigni GE, Arnone R et al (1998) Subcutaneous administration of a depot gonadotropin-releasing hormone agonist induces profound reproductive axis suppression in women. *Fertil Steril* 69(3):443–449. https://doi.org/10.1016/s0015-0282(97)00553-0
2. Hemrika DJ, Slaats EH, Schoemaker J (1994) The response of the pituitary-ovarian axis to pulsatile administration of gonadotropin-releasing hormone in long-term oral contraceptive users. *Am J Obstet Gynecol* 170(2):462–468. https://doi.org/10.1016/s0002-9378(94)70212-8
3. Kim MJ, Kim CR, Park CS et al (2023) Batteryless implantable device with built-in mechanical clock for automated and precisely timed drug administration. *Proc Natl Acad Sci USA* 120(51): e2315824120. https://doi.org/10.1073/pnas.2315824120
4. Knox ED, Stimmel GL (2004) Clinical review of a long-acting, injectable formulation of risperidone. *Clin Ther* 26(12): 1994–2002. https://doi.org/10.1016/j.clinthera.2004.12.009
5. Myung N, Kang HW (2024) Local dose-dense chemotherapy for triple-negative breast cancer via minimally invasive implantation of 3D printed devices. *Asian J Pharm Sci* 19(1):100884. https://doi.org/10.1016/j.ajps.2024.100884
6. Pandit V, Kumar A, Ashawat MS et al (2017) Recent advancement and technological aspects of pulsatile drug delivery system−a laconic review. *Curr Drug Targets* 18(10):1191–1203. https://doi.org/10.2174/1389450117666160208144343
7. Rajput A, Pingale P, Telange D et al (2024) A current era in pulsatile drug delivery system: drug journey based on chronobiology. *Heliyon* 10(10):e29064. https://doi.org/10.1016/j.heliyon.2024.e29064
8. Vela Ramirez JE, Sharpe LA, Peppas NA (2017) Current state and challenges in developing oral vaccines. *Adv Drug Deliv Rev* 114:116–131. https://doi.org/10.1016/j.addr.2017.04.008
9. D'Amico C, Fontana F, Cheng RY et al (2021) Development of vaccine formulations: past, present, and future. *Drug Deliv Transl Res* 11(2):353–372. https://doi.org/10.1007/s13346-021-00924-7
10. Ashok A, Brison M, LeTallec Y (2017) Improving cold chain systems: challenges and solutions. *Vaccine* 35(17):2217–2223. https://doi.org/10.1016/j.vaccine.2016.08.045
11. Zheng ZC, Diaz-Arévalo D, Guan HB et al (2018) Noninvasive vaccination against infectious diseases. *Hum Vaccin Immunother* 14(7):1717–1733. https://doi.org/10.1080/21645515.2018.1461296
12. Bloom BR (1989) Vaccines for the third world. *Nature* 342(6246):115–120. https://doi.org/10.1038/342115a0
13. Baryakova TH, Pogostin BH, Langer R et al (2023) Overcoming barriers to patient adherence: the case for developing innovative drug delivery systems. *Nat Rev Drug Discov* 22(5): 387–409. https://doi.org/10.1038/s41573-023-00670-0
14. Zhang YM, Liu F, Zhang YH et al (2023) Self-powered, light-controlled, bioresorbable platforms for programmed drug delivery. *Proc Natl Acad Sci USA* 120(11):e2217734120. https://doi.org/10.1073/pnas.2217734120
15. Timko BP, Arruebo M, Shankarappa SA et al (2014) Near-infrared-actuated devices for remotely controlled drug delivery. *Proc Natl Acad Sci USA* 111(4):1349–1354. https://doi.org/10.1073/pnas.1322651111
16. Hoare T, Santamaria J, Goya GF et al (2009) A magnetically triggered composite membrane for on-demand drug delivery. *Nano Lett* 9(10):3651–3657. https://doi.org/10.1021/nl9018935
17. Joo H, Lee Y, Kim J et al (2021) Soft implantable drug delivery device integrated wirelessly with wearable devices to treat fatal seizures. *Sci Adv* 7(1):eabd4639. https://doi.org/10.1126/sciadv.abd4639
18. Koo J, Kim SB, Choi YS et al (2020) Wirelessly controlled, bioresorbable drug delivery device with active valves that exploit electrochemically triggered crevice corrosion. *Sci Adv* 6(35): eabb1093. https://doi.org/10.1126/sciadv.abb1093
19. Prescott JH, Lipka S, Baldwin S et al (2006) Chronic, programmed polypeptide delivery from an implanted, multireservoir microchip device. *Nat Biotechnol* 24(4):437–438. https://doi.org/10.1038/nbt1199
20. Wang ML, Yeon P, Mofidfar M et al (2025) A wireless implantable closed-loop electrochemical drug delivery system. *IEEE Trans Biomed Circuits Syst* 19(4):777–790. https://doi.org/10.1109/TBCAS.2024.3507022
21. Pons-Faudoa FP, Ballerini A, Sakamoto J et al (2019) Advanced implantable drug delivery technologies: transforming the clinical landscape of therapeutics for chronic diseases. *Biomed Microdevices* 21(2):47. https://doi.org/10.1007/s10544-019-0389-6
22. Yoon H, Dagdeviren C (2025) Towards device technologies non-invasive to our daily lives. *Nat Commun* 16(1):1027. https://doi.org/10.1038/s41467-025-56423-7
23. Amssoms K, Born PA, Beugeling M et al (2018) Ovalbumin-containing core-shell implants suitable to obtain a delayed IgG1 antibody response in support of a biphasic pulsatile release profile in mice. *PLoS ONE* 13(8):e0202961. https://doi.org/10.1371/journal.pone.0202961
24. Grayson ACR, Choi IS, Tyler BM et al (2003) Multi-pulse drug delivery from a resorbable polymeric microchip device. *Nat Mater* 2(11):767–772. https://doi.org/10.1038/nmat998
25. Guarecuco R, Lu J, McHugh KJ et al (2018) Immunogenicity of pulsatile-release PLGA microspheres for single-injection vaccination. *Vaccine* 36(22):3161–3168. https://doi.org/10.1016/j.vaccine.2017.05.094
26. Stevenson CL, Santini JT, Langer R (2012) Reservoir-based drug delivery systems utilizing microtechnology. *Adv Drug Deliv Rev* 64(14):1590–1602. https://doi.org/10.1016/j.addr.2012.02.005
27. Fredenberg S, Wahlgren M, Reslow M et al (2011) The mechanisms of drug release in poly(lactic-co-glycolic acid)-based drug delivery systems: a review. *Int J Pharm* 415(1–2):34–52. https://doi.org/10.1016/j.ijpharm.2011.05.049
28. World Health Organization (1997) Rabies post-exposure treatment. https://www.who.int/publications/i/item/who-wer7220 [Accessed on 20 March 2025]
29. Bock H, Löscher T, Scheiermann N et al (1995) Accelerated schedule for hepatitis B immunization. *J Travel Med* 2(4): 213–217. https://doi.org/10.1111/j.1708-8305.1995.tb00661.x
30. Terrault NA, Lok ASF, McMahon BJ et al (2018) Update on prevention, diagnosis, and treatment of chronic hepatitis B: AASLD 2018 hepatitis B guidance. *Hepatology* 67(4): 1560–1599. https://doi.org/10.1002/hep.29800
31. Mahapatro A, Kulshrestha AS (2008) Polymers for Biomedical Applications. American Chemical Society, USA. https://doi.org/10.1021/BK-2008-0977
32. Christman KL (2019) Biomaterials for tissue repair. *Science*

363(6425):340–341.
https://doi.org/10.1126/science.aar2955
33. Lee SH, Park M, Park CG et al (2012) Microchip for sustained drug delivery by diffusion through microchannels. *AAPS PharmSciTech* 13(1):211–217.
https://doi.org/10.1208/s12249-011-9743-6
34. Park M, Park CG, Lee SH et al (2012) Polymeric tube-shaped devices with controlled geometry for programmed drug delivery. *Macromol Res* 20(9):960–967.
https://doi.org/10.1007/s13233-012-0140-0
35. Ji HB, Kim SN, Lee SH et al (2020) Soft implantable device with drug-diffusion channels for the controlled release of diclofenac. *J Control Release* 318:176–184.
https://doi.org/10.1016/j.jconrel.2019.12.022
36. Ji HB, Hong JY, Kim CR et al (2022) Microchannel-embedded implantable device with fibrosis suppression for prolonged controlled drug delivery. *Drug Deliv* 29(1):489–498.
https://doi.org/10.1080/10717544.2022.2032873
37. Shin JH, Min BI (2024) A study on radioprotective effects of folic acid and α-tocopherol mixture against marine radioactive contamination. *J Korean Soc Mar Environ Saf* 30(5):387–395.
https://doi.org/10.7837/kosomes.2024.30.5.387
38. Kundu J, Riajul Wahab SM, Kundu JK et al (2012) Tob1 induces apoptosis and inhibits proliferation, migration and invasion of gastric cancer cells by activating Smad4 and inhibiting β-catenin signaling. *Int J Oncol* 41(3):839–848.
https://doi.org/10.3892/ijo.2012.1517
39. Aslani A, Fattahi F (2013) Formulation, characterization and physicochemical evaluation of potassium citrate effervescent tablets. *Adv Pharm Bull* 3(1):217–225.
https://doi.org/10.5681/apb.2013.036
40. Getyala A, Gangadharappa HV, Prasad MSC et al (2013) Formulation and evaluation of non-effervescent floating tablets of losartan potassium. *Curr Drug Deliv* 10(5):620–629.
https://doi.org/10.2174/1567201811310050013
41. Zuckerman, J (2023) The place of accelerated schedules for hepatitis A and B vaccinations. *Drugs* 63(17):1779–1784.
https://doi.org/10.2165/00003495-200363170-00001
42. von Halling Laier C, Gibson B, Moreno JAS et al (2019) Microcontainers for protection of oral vaccines, in vitro and in vivo evaluation. *J Control Release* 294:91–101.
https://doi.org/10.1016/j.jconrel.2018.11.030
43. Cho M, Han JK, Suh J et al (2024) Fully bioresorbable hybrid opto-electronic neural implant system for simultaneous electrophysiological recording and optogenetic stimulation. *Nat Commun* 15(1):2000.
https://doi.org/10.1038/s41467-024-45803-0
44. Kim CR, Cho YC, Lee SH et al (2022) Implantable device actuated by manual button clicks for noninvasive self-drug administration. *Bioeng Transl Med* 8(1):e10320.
https://doi.org/10.1002/btm2.10320
45. D'souza AA, Shegokar R (2016) Polyethylene glycol (PEG): a versatile polymer for pharmaceutical applications. *Expert Opin Drug Deliv* 13(9):1257–1275.
https://doi.org/10.1080/17425247.2016.1182485
46. McHugh KJ, Nguyen TD, Linehan AR et al (2017) Fabrication of fillable microparticles and other complex 3D microstructures. *Science* 357(6356):1138–1142.
https://doi.org/10.1126/science.aaf7447
47. Gasilova ER, Zamyshlyayeva OG, Semchikov YD (2011) Conformations of poly(methyl methacrylates) end-capped with pentafluorophenyl groups. *Int J Polym Anal Charact* 16(6):349–359.
https://doi.org/10.1080/1023666X.2011.595958
48. Hodge JG, Zamierowski DS, Robinson JL et al (2022) Evaluating polymeric biomaterials to improve next generation wound dressing design. *Biomater Res* 26(1):50.
https://doi.org/10.1186/s40824-022-00291-5
49. Marano S, Laudadio E, Minnelli C et al (2022) Tailoring the barrier properties of PLA: a state-of-the-art review for food packaging applications. *Polymers* 14(8):1626.
https://doi.org/10.3390/polym14081626
50. Sarmadi M, Ta C, VanLonkhuyzen AM et al (2022) Experimental and computational understanding of pulsatile release mechanism from biodegradable core-shell microparticles. *Sci Adv* 8(28):eabn5315.
https://doi.org/10.1126/sciadv.abn5315
51. de Queiroz NMGP, Marinho FV, de Araujo ACVSC et al (2021) MyD88-dependent BCG immunotherapy reduces tumor and regulates tumor microenvironment in bladder cancer murine model. *Sci Rep* 11(1):15648.
https://doi.org/10.1038/s41598-021-95157-6
52. Best JH, Abbass I, Tominna L et al (2020) Dose modification of subcutaneous tocilizumab in patients with rheumatoid arthritis. *Am Health Drug Benefits* 13(2):72–73
53. Lindenmayer JP, Eerdekens E, Berry SA et al (2004) Safety and efficacy of long-acting risperidone in schizophrenia: a 12-week, multicenter, open-label study in stable patients switched from typical and atypical oral antipsychotics. *J Clin Psychiatry* 65(8):1084–1089.
https://www.psychiatrist.com/jcp/safety-efficacy-long-acting-risperidone-schizophrenia/ [Accessed on 16 June 2025]
54. Schwartz GG, Bessac L, Berdan LG et al (2014) Effect of alirocumab, a monoclonal antibody to PCSK9, on long-term cardiovascular outcomes following acute coronary syndromes: rationale and design of the ODYSSEY Outcomes trial. *Am Heart J* 168(5):682–689.
https://doi.org/10.1016/j.ahj.2014.07.028
55. Wang N, Shi HX, Yang SD (2022) 3D printed oral solid dosage form: modified release and improved solubility. *J Control Release* 351:407–431.
https://doi.org/10.1016/j.jconrel.2022.09.023
56. Jiang L, Li B, Ma WT et al (2024) Electroactive soft bistable actuator with adjustable energy barrier and stiffness. *IEEE Trans Robot* 40:472–482.
https://doi.org/10.1109/TRO.2023.3331065
57. Jiang YK, Li YT, Liu K et al (2023) Ultra-tunable bistable structures for universal robotic applications. *Cell Rep Phys Sci* 4(5):101365.
https://doi.org/10.1016/j.xcrp.2023.101365
58. Lee SH, Piao HY, Cho YC et al (2019) Implantable multireservoir device with stimulus-responsive membrane for on-demand and pulsatile delivery of growth hormone. *Proc Natl Acad Sci USA* 116(24):11664–11672.
https://doi.org/10.1073/pnas.1906931116
59. O'Hagan DT, Rahman D, McGee JP et al (1991) Biodegradable microparticles as controlled release antigen delivery systems. *Immunology* 73(2):239–242.
https://pmc.ncbi.nlm.nih.gov/articles/PMC1384472
60. Li W, Meng JL, Ma XH et al (2022) Advanced materials for the delivery of vaccines for infectious diseases. *Biosaf Health* 4(2):95–104.
https://doi.org/10.1016/j.bsheal.2022.03.002
61. Qi YZ, Fox CB (2021) Development of thermostable vaccine adjuvants. *Expert Rev Vaccines* 20(5):497–517.
https://doi.org/10.1080/14760584.2021.1902314
62. Singh K, Chye GC (1998) Adverse effects associated with contraceptive implants: incidence, prevention and management. *Adv Contracept* 14(1):1–13.
https://doi.org/10.1023/a:1006559124829

63. Isley MM, Edelman A (2007) Contraceptive implants: an overview and update. *Obstet Gynecol Clin N Am* 34(1):73–90. https://doi.org/10.1016/j.ogc.2007.01.002
64. Allen RH, Kaunitz AM, Hickey M (2016) Hormonal contraception. In: Williams Textbook of Endocrinology (1st Ed.). *Elsevier*, p.664–693. https://doi.org/10.1016/b978-0-323-29738-7.00018-6
65. Fowler JE (2001) Patient-reported experience with the Viadur 12-month leuprolide implant for prostate cancer. *Urology* 58(3): 430–434. https://doi.org/10.1016/S0090-4295(01)01192-X
66. Chircov C, Grumezescu AM (2022) Microelectromechanical systems (MEMS) for biomedical applications. *Micromachines* 13(2):164. https://doi.org/10.3390/mi13020164
67. Sha BC, Dimov S, Griffiths C et al (2007) Micro-injection moulding: factors affecting the achievable aspect ratios. *Int J Adv Manuf Technol* 33(1):147–156. https://doi.org/10.1007/s00170-006-0579-2
68. Trotta G, Stampone B, Fassi I et al (2021) Study of rheological behaviour of polymer melt in micro injection moulding with a miniaturized parallel plate rheometer. *Polym Test* 96:107068. https://doi.org/10.1016/j.polymertesting.2021.107068
69. de Melo LP, Salmoria GV, Fancello EA et al (2017) Effect of injection molding melt temperatures on PLGA craniofacial plate properties during in vitro degradation. *Int J Biomater* 2017: 1256537. https://doi.org/10.1155/2017/1256537
70. Khoo H, Allen WS, Arroyo-Currás N et al (2024) Rapid prototyping of thermoplastic microfluidic devices via SLA 3D printing. *Sci Rep* 14(1):17646. https://doi.org/10.1038/s41598-024-68761-5
71. Wan AMD, Moore TA, Young EWK (2017) Solvent bonding for fabrication of PMMA and COP microfluidic devices. *J Vis Exp* 119:55175. https://doi.org/10.3791/55175
72. Liparoti S, Franco P, Pantani R et al (2021) Polycaprolactone/polyethylene-glycol capsules made by injection molding: a drug release modeling. *Mater Sci Eng C* 123:112036. https://doi.org/10.1016/j.msec.2021.112036
73. Khan AR, Grewal NS, Zhou C et al (2023) Recent advances in biodegradable metals for implant applications: exploring in vivo and in vitro responses. *Results Eng* 20:101526. https://doi.org/10.1016/j.rineng.2023.101526